MOLECULAR AND CELLULAR BIOLOGY, Oct. 2002, p. 6906–6920 Vol. 22, No. 19
0270-7306/02/$04.00+0 DOI: 10.1128/MCB.22.19.6906–6920.2002

Bni5p, a Septin-Interacting Protein, Is Required for Normal Septin Function and Cytokinesis in *Saccharomyces cerevisiae*

Philip R. Lee,[1] Sukgil Song,[1] Hyeon-Su Ro,[1] Chong J. Park,[1] John Lippincott,[2] Rong Li,[2] John R. Pringle,[3] Claudio De Virgilio,[3]† Mark S. Longtine,[4] and Kyung S. Lee[1]*

Laboratory of Metabolism, Center for Cancer Research, National Cancer Institute, Bethesda, Maryland 20892[1]; Department of Cell Biology, Harvard Medical School, Boston, Massachusetts 02115[2]; Department of Biology and Program in Molecular Biology and Biotechnology, University of North Carolina, Chapel Hill, North Carolina 27599[3]; and Department of Biochemistry and Molecular Biology, Oklahoma State University, Stillwater, Oklahoma 74078[4]

Received 14 March 2002/Returned for modification 23 April 2002/Accepted 1 July 2002

In the budding yeast *Saccharomyces cerevisiae*, the Cdc3p, Cdc10p, Cdc11p, Cdc12p, and Sep7p/Shs1p septins assemble early in the cell cycle in a ring that marks the future cytokinetic site. The septins appear to be major structural components of a set of filaments at the mother-bud neck and function as a scaffold for recruiting proteins involved in cytokinesis and other processes. We isolated a novel gene, *BNI5*, as a dosage suppressor of the *cdc12-6* growth defect. Overexpression of *BNI5* also suppressed the growth defects of *cdc10-1*, *cdc11-6*, and *sep7*Δ strains. Loss of *BNI5* resulted in a cytokinesis defect, as evidenced by the formation of connected cells with shared cytoplasms, and deletion of *BNI5* in a *cdc3-6*, *cdc10-1*, *cdc11-6*, *cdc12-6,* or *sep7*Δ mutant strain resulted in enhanced defects in septin localization and cytokinesis. Bni5p localizes to the mother-bud neck in a septin-dependent manner shortly after bud emergence and disappears from the neck approximately 2 to 3 min before spindle disassembly. Two-hybrid, in vitro binding, and protein-localization studies suggest that Bni5p interacts with the N-terminal domain of Cdc11p, which also appears to be sufficient for the localization of Cdc11p, its interaction with other septins, and other critical aspects of its function. Our data suggest that the Bni5p-septin interaction is important for septin ring stability and function, which is in turn critical for normal cytokinesis.

Cytokinesis in animal cells involves an actomyosin-based contractile ring, which forms late in the cell cycle and constricts the plasma membrane, resulting in the division of one cell into two cells. In the budding yeast *Saccharomyces cerevisiae*, the cleavage plane is specified early in the cell cycle, and cytokinesis involves the concerted action of actomyosin ring contraction and septum formation (5, 37, 55). Despite some differences in the morphological features and timing of certain cytokinetic events between yeast and animal cells, many of the components involved are conserved (18). In addition to the conserved involvement of the actomyosin contractile ring, it is now widely appreciated that the septins also play a critical role in cytokinesis in both yeast and animal cells.

Septins are a family of proteins that were identified first in yeast and subsequently in various other fungi and animals (for review, see references 20, 32, and 39). Septin family members possess at least 26% amino acid sequence identity. All of the known septins possess an N-terminal P-loop and other sequences conserved in the GTPase superfamily of nucleotide-binding proteins (8). In addition, at or near their C termini, most septins possess a predicted coiled-coil domain (for review, see reference 39) that may be important in protein-protein interactions.

* Corresponding author. Mailing address: Laboratory of Metabolism, Center for Cancer Research, National Cancer Institute, NIH, 9000 Rockville Pike, Bldg. 37, Rm. 3D25, Bethesda, MD 20892. Phone: (301) 496-9635. Fax: (301) 496-8419. E-mail: kyunglee@pop.nci.nih.gov or kslee@helix.nih.gov.

† Present address: Department of Medical Biochemistry, University of Geneva, Geneva, Switzerland.

In yeast, the Cdc3p, Cdc10p, Cdc11p, Cdc12p, and Sep7p (or Shs1p) septins all localize to the presumptive bud site before bud emergence and remain at the mother-bud neck until after cytokinesis (11, 21, 28, 33, 45; M. S. Longtine, unpublished observations). Recent studies have indicated that the onset of contraction of the actomyosin ring results in division of the septins between the mother cell and the daughter cells (36, 38). Following cell separation, the septins disappear from the old cleavage site. At a restrictive temperature, temperature-sensitive mutations in *CDC3*, *CDC10*, *CDC11*, or *CDC12* result in severe defects in cytokinesis and cell morphogenesis, yielding elongated, connected cells with multiple nuclei (1, 29), whereas loss of *SEP7* function leads to milder bud elongation and cytokinetic defects (11, 45). Cdc3p, Cdc10p, Cdc11p, and Cdc12p copurify and form filaments in vitro (22), and they appear to be major structural components of the filaments observed at the neck by electron microscopy (9, 10, 22), although the details of protein arrangement in the filaments are not yet clear (22, 40).

The septins are thought to function as a scaffold for the localized assembly of various proteins at the mother-bud neck (20, 26, 40), including proteins important for cytokinesis. In a septin-dependent manner, the sole yeast type II myosin, Myo1p, assembles into a ring at the incipient budding site early in the cell cycle, whereas F actin is recruited to the myosin ring only late in the cell cycle, just before spindle disassembly and actomyosin ring contraction (5, 36, 37). Hof1p (or Cyk2p) also forms a septin-dependent ring at the mother-bud neck and appears to play an important role in modulating the stability of the actomyosin ring during contraction (36) and/or in septum

formation (55). In addition to roles in cytokinesis, the yeast septins appear to be critical for diverse cellular functions, including the localization of chitin deposition (13), bud site selection (12), mother-daughter cell compartmentalization (3, 54), pheromone-induced morphogenesis (25), and the coordination of mitotic entry with morphogenesis (4, 11, 16, 42, 47).

To identify genes that are important for septin function, we sought high-copy suppressors of the *cdc12-6* growth defect. We describe here the identification and analysis of a novel gene, *BNI5*. Our data suggest that Bni5p is important for providing stability to the neck-localized septins, probably through direct interactions with Cdc11p and perhaps also the other septins.

MATERIALS AND METHODS

Strain and plasmid construction. The yeast strains and plasmids used in this study are listed in Tables 1 and 2. All strains constructed in this study were confirmed by PCR or Southern hybridization (data not shown). To visualize septin-ring or microtubule structures, a plasmid containing a *CDC10* promoter-controlled yellow fluorescence protein gene (*YFP*)-*CDC10* fusion (51) or a *TUB1* promoter-controlled *TUB1*-green fluorescent protein gene (*GFP*) fusion (53) was integrated into the indicated strains at the *LEU2* locus. Complete deletions of the *BNI5* (*bni5*Δ::*KanMX6*), *HOF1*/*CYK2* (*hof1*Δ::*His3MX6*), *CDC10* (*cdc10*Δ::*KanMX6*), *CDC11* (*cdc11*Δ::*KanMX6*), and *SEP7*/*SHS1* (*sep7*Δ::*His3MX6*) open reading frames (ORFs) were generated by the one-step gene disruption method (41). A strain expressing a *BNI5-GFP*$_2$ fusion protein under endogenous *BNI5* promoter control (KLY1737) was generated by C-terminally tagging the chromosomal copy of *BNI5* in KLY1546 with a *GFP*$_2$::*KanMX6* fragment obtained by PCR with pSK1558 (a derivative of pFA6a-KanMX6 [41] that contains one additional copy of *GFP*^{S65T} between the *Pac*I and *Bss*HII sites) as a template. Strain KLY1737 did not exhibit any detectable defects (data not shown), suggesting that Bni5p-GFP$_2$ is functional. Strain KLY1718 was generated by introducing a plasmid containing *GAL1* promoter-controlled *GST-CDC11* into strain KLY1546 before disrupting the *CDC11* ORF as described above. This strain grew well in galactose medium, but poorly in glucose medium (data not shown). To carry out localization and functional analyses of various forms of Cdc11p, both wild-type and mutant *CDC11* alleles were C-terminally tagged with a PCR fragment containing three hemagglutinin (HA) epitopes (*HA3*), cloned into the *URA3*-based integration vector pRS306 (48), and then integrated into KLY1718 at the *URA3* locus by digesting the plasmids with *Sse*8387I. Strain KLY1718 integrated with pRS306 itself was used as a control. To determine the localization efficiency of YFP Bni5p or YFP-Cdc10p fusions in wild-type and *cdc11* mutant backgrounds, plasmid pRS314 containing either *ADH1* promoter-controlled *YFP-BNI5* (pKL1900) or *CDC10* promoter-controlled *YFP-CDC10* (pKL1901) was transformed into the KLY1718-derived strains. After repressing expression of *GAL1-GST-CDC11* by growth in glucose-containing medium for various lengths of time, the localizations of these proteins were examined. YFP-Bni5p is functional, because expression of *ADH1-YFP-BNI5* suppressed the *cdc11-6* or *cdc12-6* growth defect (data not shown). To generate strain SKY1601, the *CDC3* locus in strain KLY1546 was C-terminally tagged with a PCR fragment containing nine myc epitopes (*myc9*) bridged with a TEV protease (Life Technologies, Rockville, Md.) cleavage site. Either full-length *CDC11-HA3* or truncated *cdc11-HA3* (amino acids 1 to 385) cloned in pRS306 was then integrated into SKY1601 at the *URA3* locus (as described above) to generate strains SKY1824 and SKY1825, respectively.

To construct plasmids for two-hybrid analyses, genes were amplified by PCR. For the tests of interaction between Bni5p and the septins (see Fig. 6), genomic DNA from strain S288C was used as template. Full-length *BNI5* was fused to the VP16 transcriptional activation domain (AD) in pJG4-5 as an HA fusion protein (HA tag derived from the vector), whereas full-length *CDC3*, *CDC10*, *CDC11*, and *CDC12* were cloned in-frame to the LexA DNA-binding domain (DBD) in pEG202-NLS (Origene Technologies, Rockville, Md.) (51). For the tests of interaction among the septins (see Table 5), the cloned genes were used as templates to amplify full-length or partial genes, and *Eco*RI or *Xho*I sites were included in the primers. The partial genes *CDC3-N* (amino acids 1 to 422), *CDC3-C* (amino acids 421 to 520), *CDC11-N* (amino acids 1 to 346), *CDC11-C* (amino acids 342 to 415), *CDC12-N* (amino acids 1 to 336), and *CDC12-C* (amino acids 325 to 407) were designed to include all but the predicted coiled-coil domains (the *-N* constructs) or only the predicted coiled-coil domains (the *-C* constructs), respectively. The amplified products were fused in frame to the DBD in pEG202 and to the AD in pJG4-5 by using the *Eco*RI site (*CDC3*), the *Xho*I site (*CDC10*, *CDC11*, *CDC11-N*, and *CDC12*), or the *Eco*RI-*Xho*I sites (all other constructs) of the vectors. The constructs cloned at the *Eco*RI or *Eco*RI-*Xho*I sites of pEG202 contain two additional amino acids (EF), and the constructs cloned at the *Xho*I site contain 13 additional amino acids (EFPGIRRPWRPLE) between the LexA DBD and the first amino acid of the fused protein. The

TABLE 1. Strains used in this study

Strain	Genotype	Source or reference
1783[a]	*MAT***a** *leu2-3,112 ura3-52 trp1-1 his4 can1*^{r}	35
M-1907[b]	*MAT***a**/α *cdc12-6/cdc12-6 ura3-52/ura3-52 lys2-801/lys2-801 leu2-Δ1/leu2-Δ1 his3-Δ200/his3-Δ200 trp1-Δ63/trp1-Δ63*	This study
KLY1546[c]	*MAT***a** *his3-11,15 leu2-3,112 trp1-1 ura3*	Laboratory stock
KLY1548[c]	*MAT*α *his3-11,15 leu2-3,112 trp1-1 ura3*	Laboratory stock
KLY1415[d]	KLY1548 *cdc3-6*	This study
KLY1798[d]	KLY1546 *cdc10-1*	This study
KLY1419[d]	KLY1546 *cdc11-6*	This study
KLY1422[d]	KLY1548 *cdc12-6*	This study
KLY3937	KLY1546 *sep7*Δ::*His3MX6*	See text
KLY1350	1783 *LEU2:YFP-CDC10*	See text
KLY1940	1783 *bni5*Δ::*KanMX6*	See text
KLY1831	1783 *bni5*Δ::*KanMX6 LEU2:YFP-CDC10*	See text
KLY2177	KLY1548 *cdc3-6 bni5*Δ::*KanMX6*	See text
KLY1803	KLY1546 *cdc10-1 bni5*Δ::*KanMX6*	See text
KLY2174	KLY1546 *cdc11-6 bni5*Δ::*KanMX6*	See text
KLY2010	KLY1548 *cdc12-6 bni5*Δ::*KanMX6*	See text
KLY3941	KLY1546 *sep7*Δ::*His3MX6 bni5*Δ::*KanMX6*	See text
KLY2214	KLY1546 *cdc12-6 LEU2:YFP-CDC10*	See text
KLY2216	KLY1546 *cdc12-6 bni5*Δ::*KanMX6 LEU2:YFP-CDC10*	See text
KLY3022	1783 *hof1*Δ::*His3MX6* + pKL1754	See text
SKY2115	1783 *hof1*Δ::*His3MX6 bni5*Δ::*KanMX6* + pKL1754	See text
KLY1737	KLY1546 *BNI5-GFP*$_2$::*KanMX6*	See text
RLY292[e]	*MAT***a** *ura3-52 his3-Δ200 leu2-3,112 lys2-801 cyk2*Δ::*HIS3*	36
RLY332[e]	*MAT***a** *ura3-52 his3-Δ200 leu2-3,112 lys2-801 bar1*Δ *myo1*Δ::*HIS3*	36
KLY1715	KLY1546 *cdc10*Δ::*KanMX6*	See text
KLY1718	KLY1546 *cdc11*Δ::*KanMX6* + YCp111-GST/CDC11	See text
KLY3404	KLY1718 *URA3*:pRS306 + pKL1900	See text
KLY3405	KLY1718 *URA3:CDC11-HA3* (1–415) + pKL1900	See text
KLY3406	KLY1718 *URA3:cdc11-HA3* (1–385) + pKL1900	See text
KLY3410	KLY1718 *URA3:cdc11-HA3* (31–385) + pKL1900	See text
KLY3411	KLY1718 *URA3:cdc11-HA3* (1–200) + pKL1900	See text
KLY3412	KLY1718 *URA3*:pRS306 + pKL1901	See text
KLY3413	KLY1718 *URA3:CDC11-HA3* (1–415) + pKL1901	See text
KLY3414	KLY1718 *URA3:cdc11-HA3* (1–385) + pKL1901	See text
KLY3418	KLY1718 *URA3:cdc11-HA3* (31–385) + pKL1901	See text
KLY3419	KLY1718 *URA3:cdc11-HA3* (1–200) + pKL1901	See text
SKY1601	KLY1546 *CDC3-TEV-myc9*::*KanMX6*	See text
SKY1824	KLY1546 *CDC3-TEV-myc9*::*KanMX6 URA3:CDC11-HA3*	See text
SKY1825	KLY1546 *CDC3-TEV-myc9*::*KanMX6 URA3:cdc11-HA3* (1–385)	See text

[a] Strain 1783 is a derivative of EG123 (49).
[b] Derived by backcrossing the *cdc12-6* allele (1) repeatedly into the YEF473 (5) background.
[c] W303-1A genetic background.
[d] Derived by backcrossing the indicated *cdc* alleles (1, 29) into the KLY1546/KLY1548 background.
[e] S288C genetic background.

full-length and *-C* constructs use the original stop codons of the fused genes; the *-N* constructs use a stop codon immediately downstream of the polylinker.

Other plasmids were constructed as follows. A *Sph*I-*Sac*I fragment containing full-length *CDC3* or a *Sac*I-*Xba*I fragment containing full-length *CDC10*, *CDC11*, or *CDC12* was obtained by PCR and inserted into YCplac111 digested with the corresponding enzymes, creating plasmids pKL1061, pKL1063, pKL1064, and pKL1072, respectively. Similarly, a *Bam*HI-*Sal*I fragment containing full-length *SEP7*/*SHS1* was inserted into YCplac33 digested with the corresponding enzymes, creating plasmid pKL2184. A PCR fragment containing full-length *BNI5* was inserted into YEp351 at the *Sma*I site, creating plasmid pKL1119. pKL1120 was created by inserting a *Sac*I-*Sph*I fragment containing full-length *BNI5* into YCplac111. To express *BNI5* under *GAL1* promoter control, a *Bsp*EI-*Stu*I fragment containing the *BNI5* ORF was cloned into vector pESC-*LEU* (Stratagene, La Jolla, Calif.), creating plasmid pKL899. pKL1754 was created by inserting a *Pst*I-*Bam*HI fragment containing endogenous promoter-controlled *HOF1*/*CYK2-myc* (36) into the corresponding sites in pRS316. To construct plasmid pKL1995, which expresses full-length Bni5p fused to both N-terminal T7 and C-terminal six-His (His_6) epitope tags, a *Bsp*EI-*Xho*I fragment comprising the entire *BNI5* ORF was ligated into pET21b (Novagen, Madison, Wis.) after digestion with *Eco*RI and X*ho*I. The *Bsp*EI and *Eco*RI ends were end filled to allow blunt-end ligation. To construct plasmid pKL1993, which expresses full-length Cdc11p fused to glutathione *S*-transferase (GST), a *Bsp*EI (end filled)/*Sac*I fragment containing full-length *CDC11* was cloned into pGEX-KG (27) digested with *Bgl*II (end filled) and *Sac*I. pGEX-4T/CDC3 was generated by inserting an *Eco*RI fragment from pEG202/CDC3 (14) into the *Eco*RI site of pGEX-4T (Pharmacia, Piscataway, N.J.). pGEX-4T/CDC10, pGEX-4T/CDC11, and pGEX-4T/CDC12 were generated by inserting *Xho*I fragments from pEG202/CDC10, pEG202/CDC11, and pEG202/CDC12 (14), respectively, into the *Xho*I site of pGEX-4T.

Growth conditions and media. Yeast cell culture and transformations were carried out by standard methods (46). Yeast extract-peptone (YEP)-glucose, YEP-galactose, and synthetic media were used as appropriate. For cell cycle synchronization, *MAT***a** cells were arrested with 5 μg of α mating pheromone (Sigma, St. Louis, Mo.) per ml for 3 h at 30°C and then released into fresh growth medium. To select against cells containing *URA3* plasmids, cells were streaked onto synthetic minimal medium (SDM) supplemented with 1 g of 5-fluoroorotic acid (5-FOA) per liter (6).

Two-hybrid assays. Quantitative β-galactosidase assays were performed essentially as described previously (2) with reporter plasmid pSH18-34. The assays shown in Fig. 6 used diploid strains obtained by mating isolates of strains EGY48 and EGY194 that had been individually transformed with a pEG202-NLS-based plasmid or with a pJG4-5-based plasmid (as described above); the assays shown in Table 5 used isolates of strain EGY48 that had been cotransformed with a pEG202-based plasmid and with a pJG4-5-based plasmid.

Immunoprecipitation and immunoblotting. Cell lysates were prepared in TED buffer, composed of 40 mM Tris-Cl (pH 7.5), 0.25 mM EDTA, 1 mM dithiothreitol (DTT), 1 mM AEBSF [4-(2-aminoethyl)benzenesulfonyl fluoride] (Pefabloc; Boehringer Mannheim, Indianapolis, Ind.), 10 μg of pepstatin A per ml (Sigma), 10 μg of leupeptin per ml (Sigma), and 10 μg of aprotinin per ml (Sigma), with an equal volume of glass beads (Sigma) as described previously (50). Immunoprecipitation was carried out as described previously (51). Proteins were separated by 10% sodium dodecyl sulfate-polyacrylamide gel electrophoresis (SDS-PAGE) (2). Western blot analyses of total lysates were carried out with anti-GFP (Clontech, Palo Alto, Calif.), anti-HA.11 (Babco, Richmond, Calif.), anti-LexA (Santa Cruz Biotechnologies, Santa Cruz, Calif.), anti-T7 (Novagen), anti-GST (Clontech), anti-myc (Santa Cruz Biotechnologies), anti-Cdc28 (a gift of R. Deshaies, California Institute of Technology, Pasadena, Calif.), and anti-Clb2 (a gift of D. Morgan, University of California, San Francisco, Calif.) antibodies as described previously (51), using the ECL enhanced chemiluminescence detection system (Pierce, Rockford, Ill.).

Preparation of recombinant proteins and in vitro protein-protein interaction studies. Recombinant T7-Bni5p-His_6, GST, GST-Cdc3p, GST-Cdc10p, GST-Cdc11p, and GST-Cdc12p fusion proteins were expressed from plasmids pKL1995, pGEX-KG, pGEX-4T/CDC3, pGEX-4T/CDC10, pKL1993, pGEX-4T/CDC11, and pGEX-4T/CDC12 in *Escherichia coli*. T7-Bni5p-His_6 was partially purified with the use of a Ni-nitrilotriacetic acid column (Qiagen, Valencia, Calif.) according to the manufacturer's protocol, and GST or GST-septins were purified by using glutathione-Sepharose beads (Sigma). In addition, T7-Bni5p-His_6 was synthesized in vitro by using the T7-coupled rabbit reticulocyte system (Promega, Madison, Wis.). To investigate the interaction between Bni5p and the septins, in vitro-translated, ^{35}S-labeled T7-Bni5p-His_6 was added to either bead-bound GST-septins or bead-bound GST as a control, and then the mixture was incubated in a binding buffer (1× phosphate-buffered saline containing 0.5% NP-40) for 1 h at 4°C. The resin was then washed five times with the binding buffer. Bound proteins were eluted by boiling in SDS-PAGE sample buffer and then analyzed by autoradiogram after SDS-PAGE. To further investigate the interaction between Bni5p and Cdc11p, T7-Bni5p-His_6 partially purified from *E. coli* was added to either bead-bound GST-Cdc11p or bead-bound GST, and then the mixture was incubated in a binding buffer as described above. Bound Bni5p was separated by SDS-PAGE and detected by immunoblotting with anti-T7 (Novagen) or anti-GST (Clontech) antibodies.

TABLE 2. Plasmids used in this study

Name	Description[a]	Source or reference
pEG202-NLS	2μ, *HIS3*, *LexA* DBD	Origene Technologies, Rockville, Md.
pGEX-KG	GST fusion expression vector	27
pJG4-5	2μ, *TRP1,* transcriptional AD	2
pRS314	*CEN TRP1*	48
pRS316	*CEN URA3*	48
YCplac33	*CEN URA3*	24
YCplac111	*CEN LEU2*	24
YEp351	2μ, *LEU2*	30
YCp111-GST/CDC11	*CEN LEU2 GAL1-GST-CDC11*	22
pKL899	*CEN LEU2 GAL1-BNI5*	See text
pKL1061	YCplac111, *CDC3*	See text
pKL1063	YCplac111, *CDC10*	See text
pKL1064	YCplac111, *CDC11*	See text
pKL1072	YCplac111, *CDC12*	See text
pKL2184	YCplac33, *SEP7*/*SHS1*	See text
pKL1119	YEp351, *BNI5*	See text
pKL1120	YCplac111, *BNI5*	See text
pKL1754	pRS316, *HOF1*/*CYK2-myc*	See text
pKL1900	pRS314, *ADH-YFP-BNI5*	See text
pKL1901	pRS314, *YFP-CDC10*	See text
pKL1993	*GST-CDC11*	See text
pKL1995	*T7-BNI5-*His_6	See text
pGEX-4T/CDC3	*GST-CDC3*	See text
pGEX-4T/CDC10	*GST-CDC10*	See text
pGEX-4T/CDC11	*GST-CDC11*	See text
pGEX-4T/CDC12	*GST-CDC12*	See text

[a] 2μ indicates high-copy plasmids, and *CEN* indicates low-copy plasmids.

Cell staining and immunofluorescence microscopy. To visualize plasma membranes, cells were stained with DiI (Molecular Probes, Eugene, Oreg.) as described previously (36). To determine whether septa were formed between the cell bodies, chitin was stained as described previously (36) with Calcofluor (Fluorescent Brightener 28; Sigma), and 100-nm-interval serial sections were obtained with either a Bio-Rad MRC 1024 confocal scan head mounted on a Nikon Optiphot microscope with a ×60 planapochromat lens or a Leica TCS spectrophotometer confocal microscope. Indirect immunofluorescence was performed as described previously (34). Briefly, cells were fixed with 3.7% formaldehyde, and Cdc11p was visualized with an anti-Cdc11p antibody (Santa Cruz Biotechnologies) and a rhodamine-conjugated anti-rabbit immunoglobulin G (IgG) secondary antibody. Localization of GFP- or YFP-fused proteins was examined after fixing cells as described above. Similar results were obtained with unfixed cells. DNA was stained with 4′,6′-diamidino-2-phenylindole (DAPI).

Time-lapse imaging. Cells were grown overnight in selective medium and placed on agarose pads as described previously (56). Living cells were imaged at room temperature on an Eclipse E600 microscope with differential interference contrast (DIC) optics and a Nikon 100/1.40 oil immersion objective. Images of Bni5p-GFP and Tub1p-GFP were collected through a neutral density filter with a value of 8 every 1 min with 0.8 s of exposure to fluorescent light by using a cooled RTE/CCD 782Y Interline camera (Princeton Instruments, Trenton, N.J.). The shutter was controlled automatically with a D122 shutter driver (UniBlitz, Rochester, N.Y.) and WinView 1.6.2 software (Princeton Instruments).

RESULTS

Isolation of *BNI5* as a dosage suppressor of a septin temperature-sensitive mutant. To identify proteins that interact with the septins, we screened a yeast genomic high-copy plas-

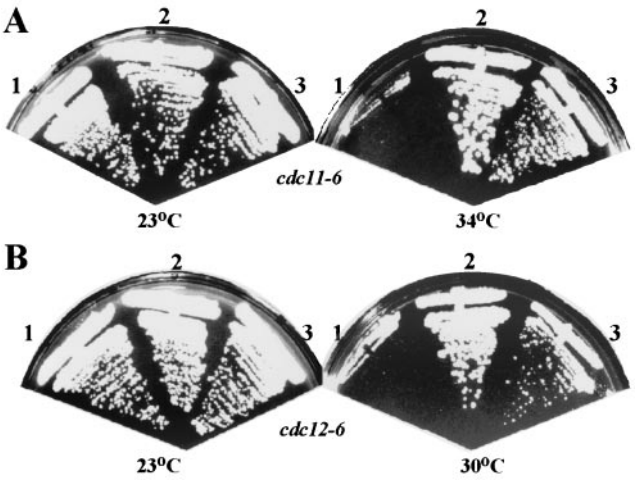

FIG. 1. Suppression of the *cdc11-6* and *cdc12-6* growth defects by overexpression of *BNI5.* (A) Strain KLY1419 (*cdc11-6*) carrying a control vector (YCplac111) (no. 1), a low-copy-number *CDC11* plasmid (pKL1064) (no. 2), or a multicopy *BNI5* plasmid (pKL1119) (no. 3) was streaked onto YEP-glucose plates and grown at the indicated temperatures for 3 days. (B) Similar tests were performed with the *cdc12-6* strain KLY1422 carrying plasmid YCplac111 (no. 1), pKL1072 (*CDC12*) (no. 2), or pKL1119 (*BNI5*) (no. 3).

mid library (13) for genes able to suppress the temperature-sensitive lethality of a *cdc12-6* mutant (strain M-1907). Initial screening at 37°C yielded no suppressing plasmids that did not contain a septin gene. However, we had found previously that overexpression of the *GIN4* gene restored viability to a septin temperature-sensitive strain at a semipermissive temperature but not at 37°C (40). Thus, we screened an additional ~100,000 transformants of strain M-1907 for growth at 32°C, recovering 30 plasmids that permitted growth at 32°C but not at 37°C. Sequencing of the ends of the inserts in these plasmids identified seven different genomic regions. Three plasmids that showed very good suppression had a region of overlap spanning nucleotides 323823 to 321482 of chromosome XIV. This region contains a single complete ORF of 1,347 bp (*YNL166C*), suggesting that overexpression of *YNL166C* was responsible for the observed suppression. This evidence and other data discussed below led us to rename *YNL166C* as "*BNI5*" (for Bud Neck Involved 5).

Next, we asked if overexpression of *BNI5* could suppress the temperature-sensitive growth defects of other septin mutants. Indeed, overexpression of *BNI5* either from a high-copy plasmid or under control of the *GAL1* promoter suppressed the *cdc10-1*, *cdc11-6,* and *sep7*Δ mutants, in addition to the *cdc12-6* mutant (Fig. 1 and Table 3). In contrast, no suppression of a *cdc3-6* mutant was detected at several temperatures examined (Table 3). It is noteworthy that overexpression of *BNI5* resulted in better suppression of the septin mutants tested than did overexpression of *GIN4* (M. Longtine, unpublished data), which was previously shown to have a positive role in septin organization (40). These data suggest that Bni5p has a positive role in septin function.

BNI5 is predicted to encode a novel protein of 50 kDa that has no obvious homologues identified as yet in other organisms. In addition, Bni5p contains no currently recognizable functional motifs, except for three possible coiled-coil regions (for review, see reference 43) at amino acids 4 to 29, 161 to 183, and 363 to 383. Interestingly, both a Bni5p-GFP_2 fusion protein expressed in *S. cerevisiae* (see Fig. 4C, below) and a T7-Bni5p-His_6 fusion protein, either expressed in *E. coli* or translated in vitro in reticulocyte extracts (see Fig. 7B and C, below), migrated much more slowly than expected during SDS-PAGE (apparent molecular masses of 137 and 85 kDa, respectively, in contrast to the predicted masses of 102 and 52 kDa).

Loss of *BNI5* function results in a partially penetrant defect in cytokinesis. To investigate the function of Bni5p, we deleted *BNI5* in a strain that expresses an integrated copy of *YFP-CDC10* under control of the normal *CDC10* promoter. The resulting strain (KLY1831) grew at normal rates at 23°C and had mild, but detectable, growth rate defects at 30 and 37°C (data not shown). After growth at 23°C, a small fraction of KLY1831 cells exhibited connected cells, occasionally with slightly elongated cell bodies. Following 12 h of growth at 37°C and sonication, ~30% of KLY1831 cells were connected as short chains and/or displayed cell bodies that were more elongated than those of the wild type (Fig. 2A). In almost all cases, cells with normal morphology appeared also to have normal septin organization, as judged by the YFP-Cdc10p fluorescence signals. In contrast, most of the morphologically abnormal cells either lacked neck-localized YFP-Cdc10p (Fig. 2A, arrows) or displayed aberrantly organized YFP-Cdc10p structures (Fig. 2A, barbed arrows). In some cases, the aberrant septin structures appeared as a set of bars parallel to the mother-bud axis. Immunostaining with an anti-Cdc11p antibody revealed that the aberrant structures also contained Cdc11p (Fig. 2B) and thus, presumably, the other septins as well. Similar septin bars have been observed in cells carrying mutations in *GIN4*, *CLA4*, or *NAP1*, genes whose products appear to be involved in septin function and organization (40, 42).

To determine whether the connected cell morphology results from a defect in cytokinesis or in cell separation, *bni5*Δ cells were grown at 37°C, sonicated, and stained with DiI to reveal the plasma membrane. In this assay, approximately 50% (n = 90) of internal mother-bud necks of connected cells with three or more cell bodies appeared to have a shared cytoplasm (Fig. 2C). *bni5*Δ cells were also stained with Calcofluor to assay for primary septum formation in the internal necks of cells with three or more cell bodies. Serial optical sectioning with a confocal microscope revealed discontinuous chitin deposition in ~90% of such necks (n = 110) (Fig. 2D), indicating defective primary septum formation. Together, these observations suggest that Bni5p plays a role in cytokinesis. Because the septins are essential for cytokinesis and septin structures are frequently abnormal in *bni5*Δ mutant cells, it is likely that the observed cytokinesis defects in *bni5*Δ strains are related to the abnormal septin organization.

Exacerbation by *bni5*Δ of septin and *hof1* mutant defects. To further examine the interaction of Bni5p and the septins, a *BNI5* deletion was introduced into *cdc3-6*, *cdc10-1*, *cdc11-6*, *cdc12-6,* and *sep7*Δ mutants. When cultured at temperatures that are normally semipermissive for these septin mutations, all double-mutant cells exhibited severely elongated buds and an apparent exacerbation of the cytokinesis defects (Fig. 3A). Compared to *bni5*Δ and septin single-mutant strains, *bni5*Δ

TABLE 3. Suppression of septin mutants by *BNI5*[a]

Mutant	Plasmid type	Degree of suppression on growth medium	
		YEPD	YEPG
cdc3-6	Vector	−	−
	2μ-*BNI5*	−	−
	GAL1-BNI5	−	−
	CDC3	+4	+4
cdc10-1	Vector	−	−
	2μ-*BNI5*	+1	+1
	GAL1-BNI5	−	+1
	CDC10	+4	+4
cdc11-6	Vector	−	−
	2μ-*BNI5*	+2	+2
	GAL1-BNI5	−	+2
	CDC11	+4	+4
cdc12-6	Vector	−	−
	2μ-*BNI5*	+2	+2
	GAL1-BNI5	−	+2
	CDC12	+4	+4
*sep7*Δ	Vector	−	−
	2μ-*BNI5*	+1	+1
	GAL1-BNI5	−	+1
	SEP7	+4	+4

[a] The *cdc3-6, cdc10-1,* and *cdc12-6* transformants were tested at 30°C, whereas the *cdc11-6* and *sep7*Δ transformants were tested at 34 and 37°C, respectively. The *cdc3-6* transformant was also tested at several other temperatures without detecting any suppression (data not shown). The degree of suppression of the growth defects is scored on an arbitrary scale from +1 to +4. −, no suppression. Strains: *cdc3-6,* KLY1415; *cdc10-1,* KLY1798; *cdc11-6,* KLY1419; *cdc12-6,* KLY1422; *sep7*Δ, KLY3937. Plasmids: 2μ-*BNI5,* pKL1119; *GAL1-BNI5,* pKL899; *CDC3,* pKL1061; *CDC10,* pKL1063; *CDC11,* pKL1064; *CDC12,* pKL1072; *SEP7,* pKL2184. Note that in this strain background, the *sep7*Δ mutation produces a significant growth defect with a chained-cell morphology at 37°C. The growth media used were YEP-glucose (YEPD) and YEP-galactose (YEPG).

*cdc10-1, bni5*Δ *cdc11-6*, *bni5*Δ *cdc12-6*, and *bni5*Δ *sep7*Δ double-mutant strains, but not a *bni5*Δ *cdc3-6* double-mutant strain, also exhibited enhanced growth defects at elevated temperatures (Fig. 3C and data not shown). We also compared the localization of YFP-Cdc10p in *cdc12-6* and *bni5*Δ *cdc12-6* mutants. In the *cdc12-6* strain, YFP-Cdc10p appeared to localize normally at 23°C, and approximately 80% of the cells possessed neck-localized YFP-Cdc10p after 3 h at 30°C (Fig. 3B and D). In contrast, in the *bni5*Δ *cdc12-6* double-mutant strain, YFP-Cdc10p was often aberrantly localized at 23°C and was largely absent from the necks after 3 h at 30°C (Fig. 3B and D). Together, these observations suggest that Bni5p contributes to the maintenance or stability of neck-localized septins.

We also tested for genetic interactions between Bni5p and other cellular components known to be important for cytokinesis. Loss of *HOF1* function leads to a rapid disassembly of the actomyosin ring during its contraction, sometimes causing incomplete cytokinesis, whereas overexpression of *HOF1* can block cytokinesis, probably by disrupting septin localization to the neck (31, 36, 55). Consistent with a role for Bni5p in cytokinesis, *bni5*Δ was synthetically lethal with a *hof1*Δ mutation (Fig. 3E). Tetrad analysis of a diploid strain heterozygous for the *bni5*Δ and *hof1*Δ mutations also showed that *bni5*Δ *hof1*Δ double-mutant spores were incapable of forming colonies at 23°C. Microscopic analysis of the double-mutant segregants (Fig. 3F) revealed that they produced several interconnected cell bodies before cessation of growth, which appeared to result from cell lysis. In contrast, a *bni5*Δ *myo1*Δ double-mutant strain did not exhibit any detectable synthetic defect (data not shown), suggesting that Bni5p and Myo1p may function in the same pathway.

Cell cycle-dependent expression and localization of Bni5p. To investigate the localization of Bni5p, the chromosomal *BNI5* gene was tagged at its C-terminal end with two tandem copies of GFP sequences. The tagged Bni5p appeared to be fully functional (see Materials and Methods). Microscopic observation of asynchronously growing cells revealed a band of Bni5p-GFP at the mother-bud neck in most budded cells (Fig. 4A). However, Bni5p was not detectably localized in most unbudded cells or in some cells with nascent buds, as well as in some large-budded cells (Fig. 4A). Immunostaining with an anti-Cdc11p antibody revealed that the Bni5p-GFP band corresponded approximately to that of the septins (Fig. 4B). Although the Bni5p band often appeared to occupy only a portion of the region defined by the septin staining (Fig. 4B, arrows), this appearance might just result from the greater strength of the Cdc11p signal relative to that of the Bni5p-GFP signal. Interestingly, Bni5p-GFP localization was not detected in some unbudded or nascent-budded cells, or in some large-budded cells, even when the septins were clearly present (Fig. 4B, barbed arrows). These data suggest that Bni5p arrives at the bud site approximately coincident with bud emergence (and thus ~10 to 15 min later than the septins [21, 33]) and dissociates from the septin scaffold before cytokinesis.

To explore further the timing of Bni5p localization and to investigate whether the changes in localization reflect changes in Bni5p abundance, we examined Bni5p-GFP levels and localization in a synchronous culture. Bni5p-GFP levels were low in the α-factor-arrested cells and for 20 min after release (Fig. 4C). They then increased abruptly between 20 and 40 min and peaked at ~50 to 70 min, approximately coincident with the G_2/M peak in Clb2p levels (Fig. 4C). These observations are consistent with microarray data indicating that *BNI5* mRNA is enriched in the S phase (52; Saccharomyces Genome Database, Stanford University, Calif.). The percentage of cells with detectably localized Bni5p-GFP also increased abruptly between 20 and 40 min after release and paralleled (but perhaps lagged slightly behind) the appearance of buds (Fig. 4D). Between 70 and 90 min after release, the number of cells with detectably localized Bni5p-GFP first fell abruptly, even though the number of budded cells remained high, and then began to increase again, presumably as new buds were formed in the next cell cycle (Fig. 4D). These data support the inferences about the timing of Bni5p localization and delocalization that were made from the observations on asynchronous cells, and they also suggest that the changes in Bni5p localization may reflect, at least in part, changes in Bni5p abundance during the cell cycle.

To further explore the timing of Bni5p delocalization from the neck, we made time-lapse observations of living cells expressing both Bni5p-GFP and Tub1p-GFP. As shown in Fig. 5, the band of Bni5p disappeared abruptly, without any detectable change in diameter, 2 to 4 min before spindle disassembly. Interestingly, Bni5p localization to the neck was still apparent in the *cdc5-1* and *cdc15-2* mutants, which are defective in exit

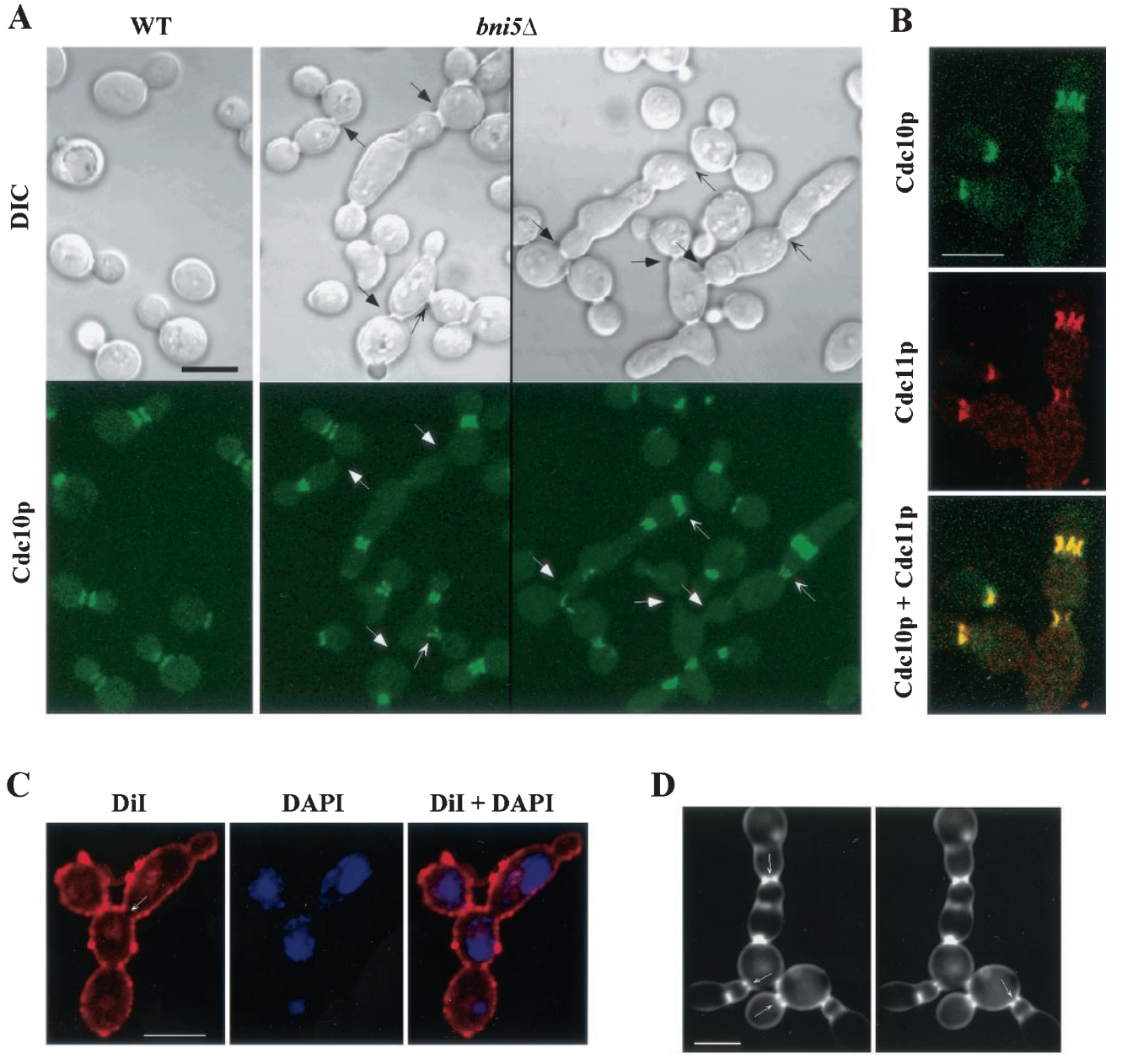

FIG. 2. Loss of *BNI5* function leads to defects in septin localization and cytokinesis. (A) Strains KLY1350 (*BNI5 YFP-CDC10*) and KLY1831 (*bni5*Δ *YFP-CDC10*) grown in YEP-glucose at 23°C were shifted to 37°C for 12 h, fixed with formaldehyde, and examined by confocal microscopy. Representative morphologies are shown for each strain. Arrows indicate structures discussed in the text. WT, wild type. (B) Strain KLY1831 (*bni5*Δ *YFP-CDC10*), cultured as in panel A, was fixed with formaldehyde and subjected to immunostaining with anti-Cdc11p antibodies. (C) Strain KLY1940 (*bni5*Δ), cultured as in panel A, was fixed and stained with DiI to reveal membrane structures and stained with DAPI to visualize the DNA. The arrow indicates a neck with apparently connected cytoplasm. (D) Cells from the culture in panel C were stained with Calcofluor and subjected to confocal microscopy in 100-nm sections to investigate whether septa are formed. Arrows indicate seemingly incomplete primary septa as seen in the appropriate planes of focus. Bars, 5 μm.

from mitosis, after 3.5 h at a restrictive temperature (data not shown). Since the spindle disassembles at the onset of cytokinesis (36), these observations indicate that Bni5p delocalizes from the neck after mitotic exit has been triggered, but before the onset of cytokinesis.

Dependence of Bni5p localization on direct interaction with septins. To ask if Bni5p neck localization depends on the septins, Bni5p with an N-terminal YFP tag was expressed under control of the *ADH1* promoter in *cdc3-6*, *cdc10-1*, *cdc11-6*, and *cdc12-6* strains. Although YFP-Bni5p was clearly localized to the neck in all four strains at permissive temperature, neck localization was lost when the cultures were shifted to a nonpermissive temperature for 30 (*cdc10-1* and *cdc12-6*) or 60 (*cdc3-6* and *cdc11-6*) min (Table 4 and data not shown). We also examined Bni5p localization in the viable septin deletion mutants. A *cdc11*Δ mutant conditionally expressing *GAL-*

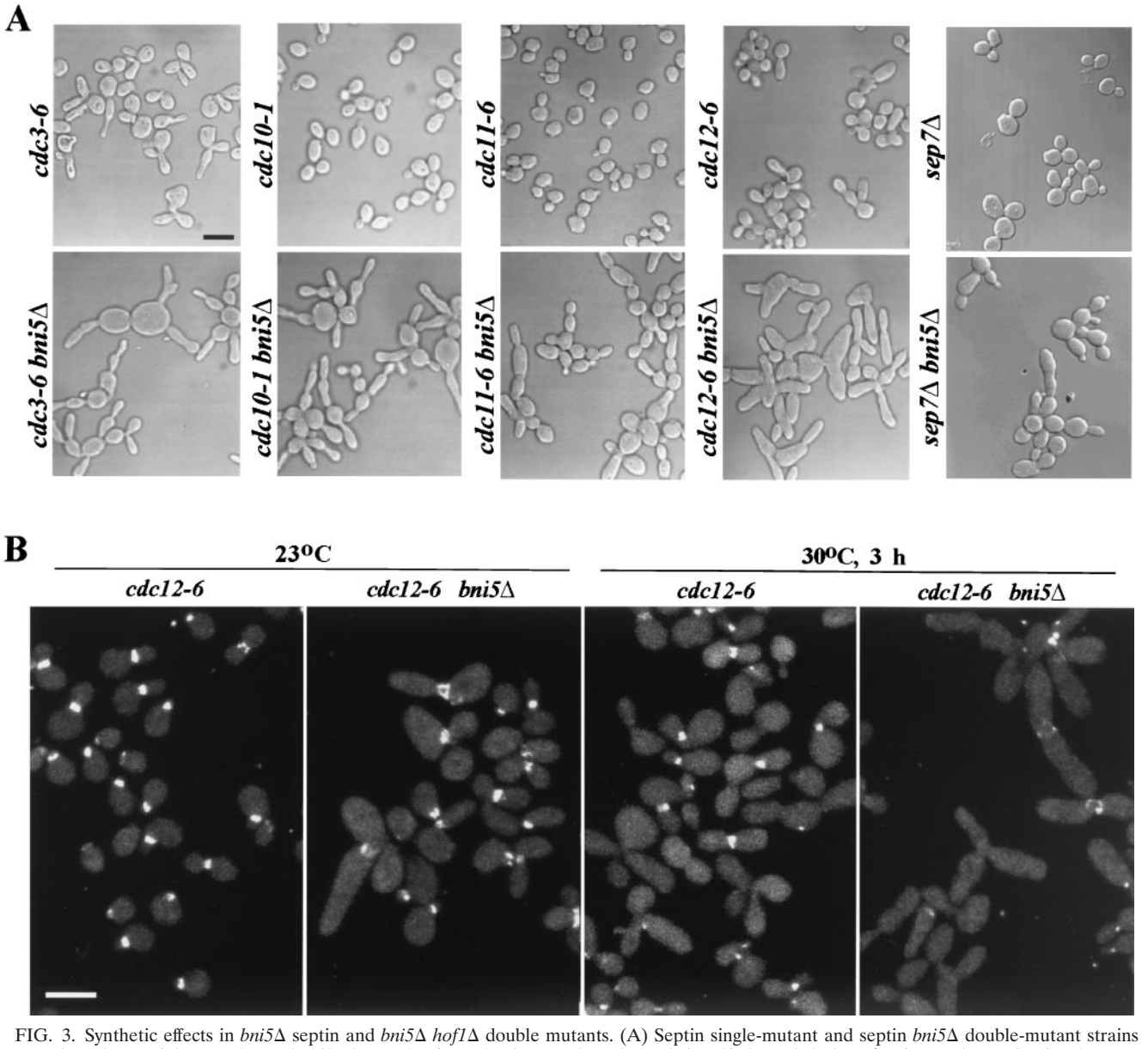

FIG. 3. Synthetic effects in *bni5*Δ septin and *bni5*Δ *hof1*Δ double mutants. (A) Septin single-mutant and septin *bni5*Δ double-mutant strains were cultured overnight at 23°C and shifted to 30°C (or 37°C for *sep7*Δ and *sep7*Δ *bni5*Δ) for 3 h before fixation and examination by DIC microscopy. Strains: *cdc3-6*, KLY1415; *cdc10-1*, KLY1798; *cdc11-6*, KLY1419; *cdc12-6*, KLY1422; *sep7*Δ, KLY3937; *cdc3-6 bni5*Δ, KLY2177; *cdc10-1 bni5*Δ, KLY1803; *cdc11-6 bni5*Δ, KLY2174; *cdc12-6 bni5*Δ, KLY2010; *sep7*Δ *bni5*Δ, KLY3941. Bar, 5 μm. (B) Strains KLY2214 (*cdc12-6 YFP-CDC10*) and KLY2216 (*cdc12-6 bni5*Δ *YFP-CDC10*) were cultured overnight at 23°C and then shifted to 30°C. Samples were fixed for microscopic analyses during growth at 23°C and 3 h after the shift to 30°C. Bar, 5 μm. (C) Strains KLY1546 (wild type) (lane 1), KLY2214 (lane 2), and KLY2216 (lane 3) were cultured overnight. These cultures were serially diluted, spotted on YEP-glucose (YEPD), and incubated at the indicated temperature for 3 days. (D) Quantitation of cells with YFP-Cdc10p localization at the neck as a function of time. The strains used in panel B were cultured overnight at 23°C and then shifted to 30°C. Samples were fixed for microscopic analyses during growth at 23°C and at the indicated times after the shift to 30°C. The fractions of cells with YFP-Cdc10p localization at the neck were determined by counting more than 200 cells for each sample. Cells with partially localized YFP-Cdc10p at the neck were scored as positive. (E) Synthetic lethality between *bni5*Δ and *hof1*Δ. Strains 1783 (wild type) (no. 1), KLY1940 (*bni5*Δ) (no. 2), KLY3022 (*hof1*Δ with a *HOF1*/*CYK2* plasmid) (no. 3), and SKY2115 (*bni5*Δ *hof1*Δ with the *HOF1*/*CYK2* plasmid) (no. 4) were streaked on YEPD plates with or without 5-FOA to select against the *URA3*-based plasmid. (F) Two examples of *bni5*Δ *hof1*Δ double-mutant segregants after tetrad dissection of a heterozygous diploid.

GST-CDC11 (KLY1718) was further transformed either with plasmid pKL1900 (expressing *YFP-BNI5* under *ADH1* promoter control) or with plasmid pKL1901 (expressing *YFP-CDC10* under endogenous *CDC10* promoter control), and the localization of YFP-Bni5p or YFP-Cdc10p was determined upon depletion of GST-Cdc11p by a shift to glucose-containing medium. The YFP-Bni5p rings completely disappeared from the bud necks within 1 h of the shift (Fig. 6A), whereas the YFP-Cdc10p signal was stable for at least several hours under the same conditions (data not shown). In contrast, YFP-Bni5p

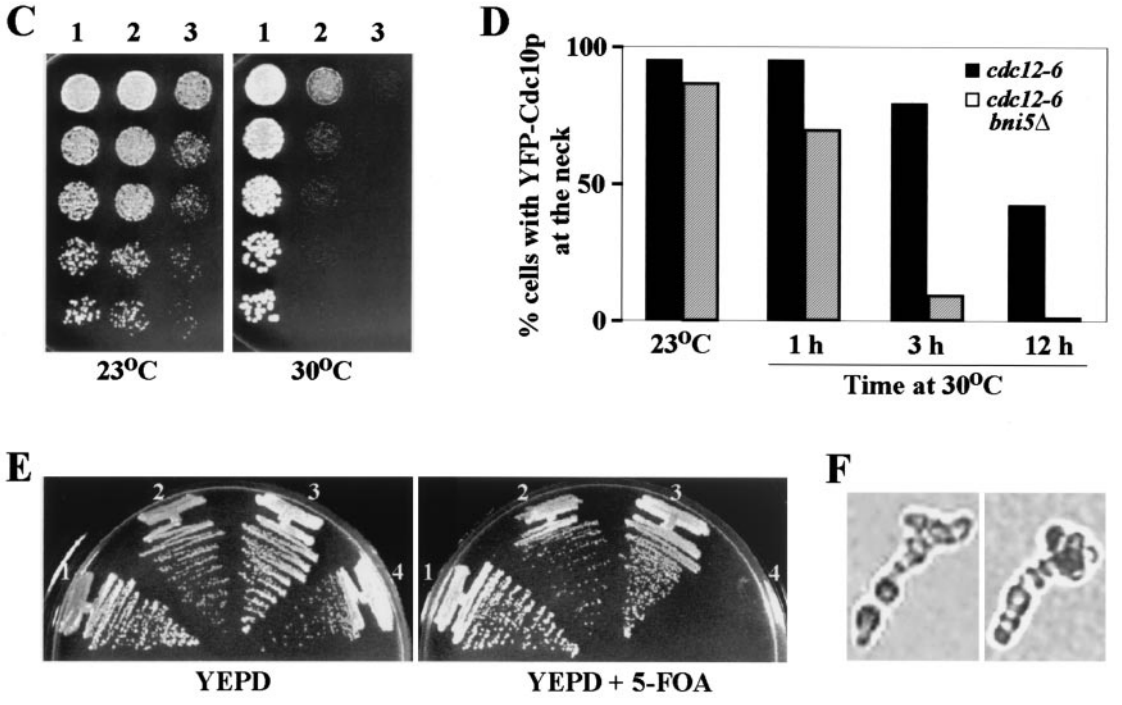

FIG. 3—*Continued.*

localized normally to the neck in *cdc10*Δ cells at 23°C (Fig. 6A), as well as in *hof1*Δ (strain RLY292) and *myo1*Δ (strain RLY332) cells (data not shown). In a *sep7*Δ mutant (strain KLY3937 containing plasmid pKL1900), the localization of YFP-Bni5p was severely impaired at temperatures from 23 to 37°C. However, at 23°C, approximately 10% of the population still exhibited normal-looking YFP-Bni5p rings (data not shown). Taken together, these observations suggest that Bni5p localization depends on the septins and perhaps particularly on Cdc11p. In addition, because the neck filaments are disorganized in a *cdc10*Δ background (22), these observations suggest that Bni5p, like Bud4p, Cdc3p, and Cdc11p (17, 22), does not depend on intact neck-filament structures for its normal localization.

We next asked if Bni5p interacts physically with Cdc11p or other septins. In two-hybrid assays, Bni5p interacted with Cdc11p and perhaps with Cdc12p, but not with Cdc3p or Cdc10p (Fig. 7A). In addition, in vitro binding studies showed that GST-Cdc11p interacted with in vitro-translated T7-Bni5p-His_6 (Fig. 7B). Under the same conditions, GST-Cdc3p, GST-Cdc10p, and GST-Cdc12p, but not GST alone, also interacted with Bni5p at a somewhat lesser level (Fig. 7B). In a second experiment, we observed that GST-Cdc11p, but not GST alone, could interact with bacterially expressed, partially purified, T7-Bni5p-His_6 (Fig. 7C). Taken together, these data support the hypothesis that Bni5p interacts directly with Cdc11p and perhaps also with the other septins.

To investigate which domain(s) of Cdc11p may be important for the interaction with Bni5p, and hence for Bni5p localization, we integrated into strain KLY1718 (*cdc11*Δ with a *GAL1-GST-CDC11* plasmid) various HA-tagged Cdc11p constructs under normal *CDC11* promoter control (Fig. 6B and C). These strains were then transformed with a plasmid expressing either *ADH1-YFP-BNI5* or *YFP-CDC10*. Cells were fixed after depleting GST-Cdc11p by growth in 2% glucose for 1 h, and the percentages of budded cells with neck-localized YFP-Bni5p or YFP-Cdc10p were determined. In strains expressing either full-length $Cdc11p^{1-415}$ or $Cdc11p^{1-385}$, YFP-Bni5p was detectable at approximately 90% of the necks in budded cells (Fig. 6D). This result is striking because $Cdc11p^{1-385}$ lacks a canonical leucine zipper motif (Leu384-X6-Leu391-X6-Leu398-X6-Leu405) that comprises about half of the 57-amino-acid coiled-coil domain predicted by the Coils program (44). In contrast, YFP-Bni5p localization was greatly diminished or abolished in the strains expressing $Cdc11p^{31-385}$ or $Cdc11p^{1-200}$ (Fig. 6D), even though these proteins were expressed at levels comparable to those of the others (Fig. 6C). Under the same condi-

TABLE 4. Septin-dependent localization of Bni5p[a]

Strain	% of budded cells with signal[b]	
	23°C	37°C for 0.5 h
Wild-type		
YFP-Cdc10p	89	91
YFP-Bni5p	76	79
cdc12-6		
YFP-Cdc10p	84	0
YFP-Bni5p	69	0

[a] Wild-type strain KLY1546 or the isogenic *cdc12-6* mutant KLY1422 was transformed either with pKL1901 (expressing *YFP-CDC10* under endogenous *CDC10* promoter control) or with pKL1900 (expressing *YFP-BNI5* under *ADH1* promoter control). The transformants were grown overnight at 23°C, and half of each culture was shifted to 37°C for 30 min before fixing the cells.

[b] For each sample, the percentage of budded cells with localized YFP-Cdc10p or YFP-Bni5p signal at the mother-bud neck was determined by examining at least 200 budded cells.

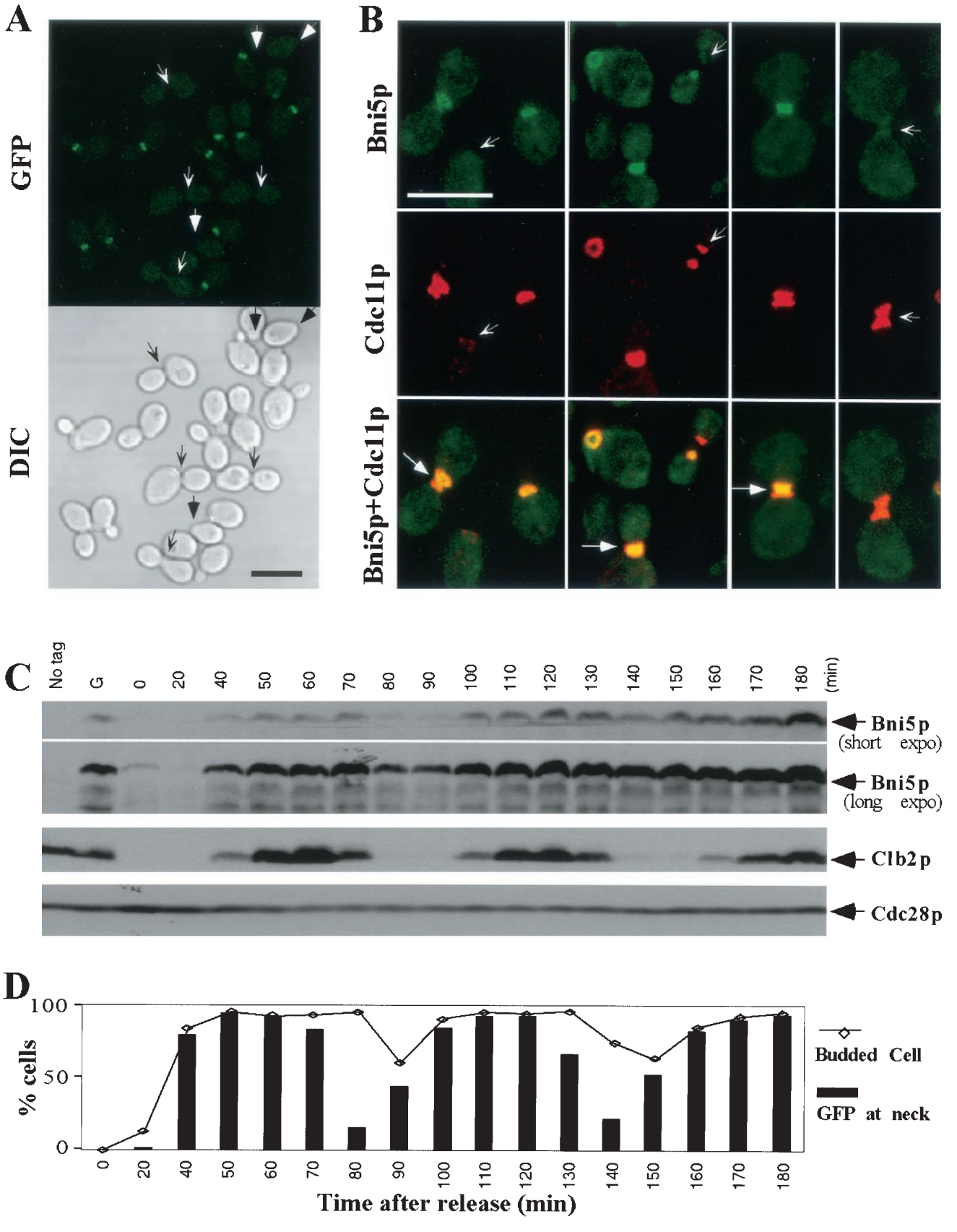
A
GFP
DIC
B
Bni5p
Cdc11p
Bni5p+Cdc11p
C
No tag
G
0
20
40
50
60
70
80
90
100
110
120
130
140
150
160
170
180
(min)
Bni5p
(short expo)
Bni5p
(long expo)
Clb2p
Cdc28p
D
% cells
100
50
0
Budded Cell
GFP at neck
Time after release (min)

TABLE 5. Two-hybrid interactions among the *S. cerevisiae* septins[a]

AD fusion	β-Galactosidase activity (Miller units) with DBD fusion[b]									
	CDC3	*CDC3-N*	*CDC3-C*	*CDC10*	*CDC11*	*CDC11-N*	*CDC11-C*	*CDC12*	*CDC12-N*	*CDC12-C*
None[c]	14	21	29	38	14	21	26	3	15	24
CDC3	5	8	27	**290**	5	13	25	**2,020**	10	**1,680**
CDC3-N	1	7	29	150	3	12	9	1	4	6
CDC3-C	4	16	25	33	7	40	11	**410**	1	**500**
CDC10	99	**390**	17	31	4	37	14	4	26	11
CDC11	**1,460**	69	160	**610**	**780**	**500**	7	**1,760**	**630**	14
CDC11-N	**350**	7	24	**250**	66	**1,640**	8	**1,760**	**570**	19
CDC11-C	12	8	56	42	5	43	12	32	20	3
CDC12	**1,630**	41	**1,600**	200	**1,150**	**1,220**	1	**1,740**	45	**1,530**
CDC12-N	**260**	**270**	39	51	**920**	**1,610**	27	**190**	13	19
CDC12-C	40	21	**700**	21	8	50	13	**120**	2	**830**

[a] Two-hybrid assays were performed as described in Materials and Methods.

[b] β-Galactosidase activities were measured on three independent isolates of each strain after growth for 16 h at 30°C in minimal medium containing 1% raffinose and 2% galactose. The average values (in Miller units) are shown. Values that are above 100 Miller units and at least sixfold higher than the corresponding control (pJG4-5 with no insert) are shown in boldface. *-N* and *-C* indicate the N- and C-terminal fragments, respectively, of the gene in question (see Materials and Methods for details).

[c] None, pJG4-5 with no insert.

tions, YFP-Cdc10p localization at the bud neck was consistently detected in all the strains (Fig. 6D). These data suggest that the N-terminal region (amino acids 1 to 385) of Cdc11p is sufficient for Bni5p localization and that the C-terminal coiled-coil domain is not involved in this event.

Apparently normal function of Cdc11p lacking the coiled-coil domain. The neck localization of Bni5p in the Cdc11p$^{1-385}$ cells suggested that Cdc11p$^{1-385}$ itself also localizes to the neck. Indeed, immunostaining revealed that Cdc11p$^{1-385}$ localized to the neck as well as did the full-length protein, whereas the other mutant Cdc11p proteins did not (Fig. 6D and E). We then examined the abilities of the Cdc11p truncation mutants to complement the *cdc11*Δ growth defect. Consistent with the localization data, Cdc11p$^{1-385}$ appeared to complement the growth defect as well as did the full-length protein, while the other truncated proteins did not (Fig. 6F). Finally, we examined whether Cdc11p$^{1-385}$ could form a complex with other septin proteins. In strains expressing a myc-tagged Cdc3p and either HA-tagged full-length Cdc11p or HA-tagged Cdc11p$^{1-385}$, immunoprecipitation with anti-HA antibodies was equally effective in coprecipitating Cdc3p-myc (Fig. 6G). This observation is consistent with the results of a matrix of two-hybrid tests involving the full-length and partial septin proteins (Table 5). In particular, although no interactions were observed with the C-terminal domain of Cdc11p, the N-terminal domain appeared to be capable of interacting with itself, with the N-terminal domain of Cdc12p, and with Cdc3p and Cdc10p. With regard to possible models of septin assembly (see Discussion), it was also of interest in these experiments that no homotypic interactions were observed with the Cdc3p constructs (although these did interact with other septins) and that the C-terminal domain of Cdc12p appeared to interact well not only with itself but also with the C-terminal domain of Cdc3p (Table 5). Taken together, these data suggest that the predicted coiled-coil domain of Cdc11p is not required for interaction with other septins, for neck localization, or for other vital aspects of Cdc11p function, and that the assembly of septin complexes involves complex interactions involving both the N- and C-terminal portions of the proteins.

DISCUSSION

Interaction of Bni5p with Cdc11p and other septins. In this study, we have performed an initial characterization of the novel *S. cerevisiae* protein Bni5p. Multiple lines of evidence indicate that Bni5p interacts with the septin array at the mother-bud neck. First, *BNI5* acts as a dosage suppressor of several different temperature-sensitive septin mutations. Second, Bni5p localizes to the neck in a septin-dependent manner. Third, deletion of *BNI5* results in partially penetrant defects in septin organization and in the septin-dependent process of cytokinesis, and double mutants containing both *bni5*Δ and a temperature-sensitive septin mutation display a phenotype that is more severe than those of the single mutants. Fourth, *bni5*Δ is synthetically lethal with deletion of *HOF1*/*CYK2*, a gene whose product appears to interact with the septins and other proteins involved in cytokinesis (31, 36, 55). Finally, both two-hybrid data and GST pull-down experiments suggest that

FIG. 4. Expression and localization of Bni5p through the cell cycle. (A) Localization of Bni5p to the neck of budded cells. Exponentially growing cells of strain KLY1737 (*BNI5-GFP$_2$*) were fixed and examined for Bni5p-GFP localization and cell morphology. Arrows, unbudded cells or cells with nascent buds without detectable Bni5p-GFP signal; barbed arrows, large-budded cells without detectable Bni5p-GFP signal. Bar, 5 μm. (B) Colocalization of Bni5p and Cdc11p. Bni5p was visualized by the GFP signal, whereas Cdc11p was detected by immunofluorescence. Barbed arrows, unbudded or large-budded cells with Cdc11p signal but no Bni5p signal; arrows, localization of Bni5p within the Cdc11p bands. Bar, 5 μm. (C and D) Levels of Bni5p and Bni5p localization in a synchronous culture. Strain KLY1737 was arrested in G_1 by α-factor treatment for 3 h and then released. At the indicated times, samples were taken to prepare total cellular proteins and to determine Bni5p localization and the presence or absence of buds after fixation. (C) Proteins were separated by 10% SDS-PAGE and analyzed by Western blotting with antibodies against GFP, Clb2p, or Cdc28p. Both short and long exposures of the Bni5p-GFP immunoblot are shown for clarity. The Cdc28p levels provide a loading control. No tag, wild-type strain KLY1546; G, asynchronously growing KLY1737 cells. (D) The percentages of budded cells and of cells showing detectable Bni5p-GFP localization were determined by counting more than 200 cells for each time point.

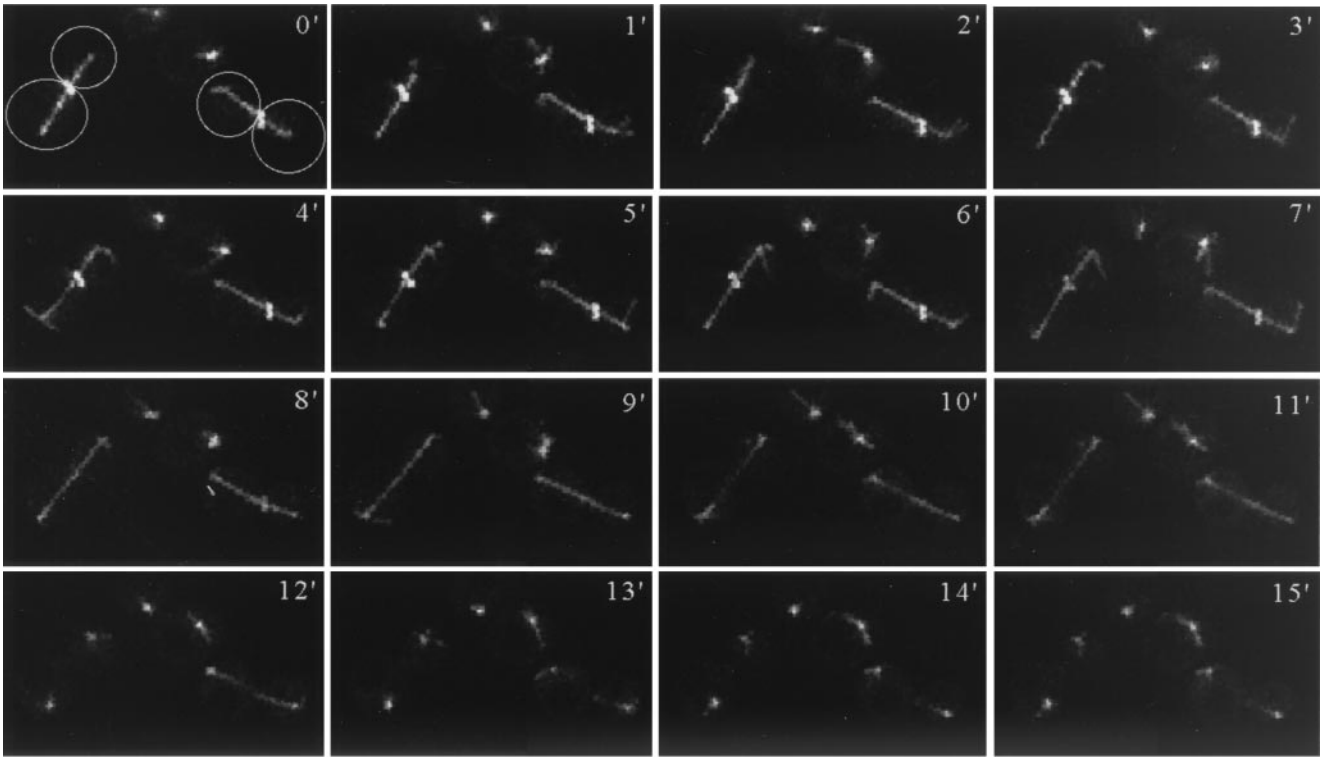

FIG. 5. Dynamics of Bni5p neck localization in relation to spindle structure. Strain KLY1737 (*BNI5-GFP*$_2$) was transformed with *TUB1-GFP* (see Materials and Methods) and then examined by time-lapse video microscopy as described in Materials and Methods. In the two cells imaged here (outlined in the first panel), Bni5p-GFP is visible as a band crossing the elongated spindle. Spindle disassembly began at 10 min in the cell on the left or 12 min in the cell on the right.

Bni5p interacts directly with Cdc11p, a suggestion supported by the observations that Bni5p is present at the neck in a *cdc10*Δ or a *sep7*Δ strain but disappears rapidly from the neck when Cdc11p is depleted in a viable *cdc11*Δ strain. The GST pull-down experiments also suggest that Bni5p may interact directly, but more weakly, with the other septins.

Although many proteins have now been shown to localize to the mother-bud neck in a septin-dependent manner (26), suggesting a scaffold function for the septin array, there are very few cases in which strong evidence exists for a specific and/or direct interaction with a particular septin. For example, although the available evidence does suggest that Bni4p interacts specifically with Cdc10p (13) and that Gin4p interacts specifically with Cdc3p (40), these putative interactions have not yet been observed with the isolated proteins. Thus, the results with Bni5p are important in suggesting that at least some proteins are recruited to the neck by direct interaction with the septins and that interaction with particular septins (e.g., Cdc11p in the case of Bni5p) may be largely responsible for the recruitment in particular cases.

Possible roles of Bni5p. Except for the possible coiled-coil domains, the sequence of Bni5p displays no known motifs or

FIG. 6. Dependence of Bni5p localization and Cdc11p function on the N-terminal portion of Cdc11p. (A) Localization of YFP-Bni5p in wild-type and viable septin deletion mutants. Wild-type strain KLY1546 and the *cdc10*Δ mutant (KLY1715), both expressing YFP-Bni5p from plasmid pKL1900, were cultured in YEP-glucose (YEPD) medium. Strain KLY1718 (*cdc11*Δ + YCp111-*GST*/*CDC11*) expressing YFP-Bni5p from plasmid pKL1900 was cultured in YEP-galactose overnight and then shifted to YEPD to repress *GAL1-GST-CDC11* expression for 1 h prior to fixation. Bar, 5 μm. (B) Structures of the Cdc11p truncations used in these analyses (see Materials and Methods). Solid box, the conserved P-loop motif; shaded box, the predicted coiled-coil domain. (C to E) Strain KLY1718 (*cdc11*Δ + YCp111-*GST*/*CDC11*) derivatives harboring various C-terminally HA-tagged Cdc11p constructs and a plasmid expressing either *YFP-CDC10* or *ADH1-YFP-BNI5* were cultured in YEP-galactose (YEPG) overnight and then shifted to YEPD medium to repress *GAL1-GST-CDC11* expression for 1 h. For each culture, total cellular lysates were prepared for Western analysis (C), and an aliquot was fixed with formaldehyde to assess Cdc10p and Bni5p localization by YFP fluorescence (D) or Cdc11p localization by immunostaining with an anti-HA antibody (D and E). Cdc10p, YFP-Cdc10p; Bni5p, YFP-Bni5p; Cdc11p, wild-type and mutant Cdc11p-HA proteins; vector, strain KLY3404 or KLY3412; 1-415, strain KLY3405 or KLY3413; 1-385, strain KLY3406 or KLY3414; 31-385, strain KLY3410 or KLY3418; 1-200, strain KLY3411 or KLY3419. For panel D, more than 200 cells with clear buds were counted for each sample. (F) Wild-type strain KLY1546 and the KLY1718 derivatives KLY3404, KLY3405, KLY3406, KLY3410, and KLY3411 were cultured overnight, serially diluted, and spotted onto either YEPG or YEPD plates at 30°C. Strains expressing either Cdc11p$^{1\text{-}415}$ or Cdc11p$^{1\text{-}385}$ grow better than the others even on YEPG, because *GAL-GST-CDC11* does not fully complement the *cdc11*Δ mutation. (G) Strains expressing myc-tagged Cdc3p together with no tagged Cdc11p (SKY1601), HA-tagged full-length Cdc11p (SKY1824), or HA-tagged Cdc11p$^{1\text{-}385}$ (SKY1825) were grown on YEPD at 30°C, and extracts were prepared as described in Materials and Methods. Proteins present in the total lysates or in the immunoprecipitates (IP) prepared with anti-HA antibody were evaluated by Western blotting with anti-myc (above) and anti-HA (below) antibodies.

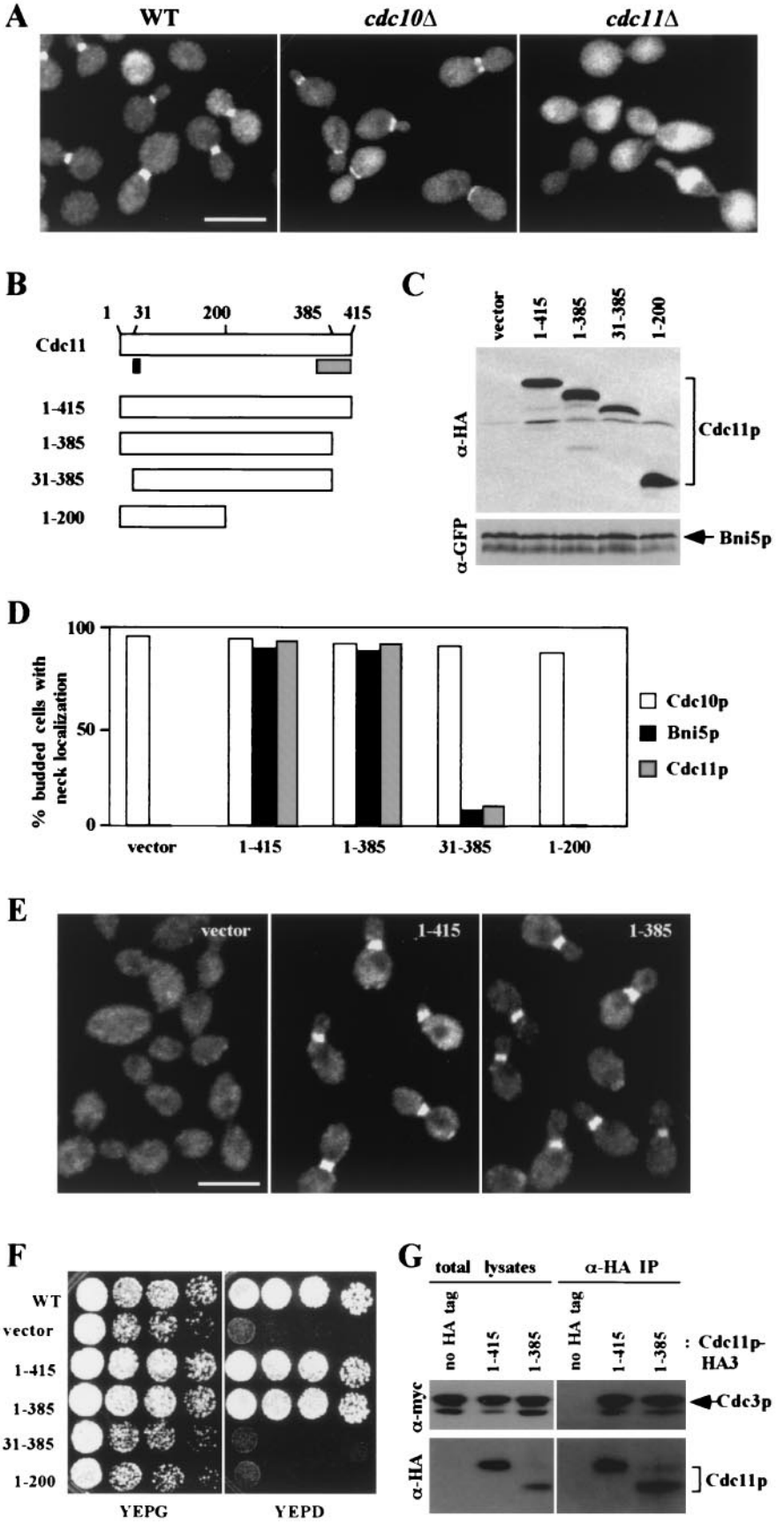
A
WT
cdc10Δ
cdc11Δ
B
1
31
200
385
415
Cdc11
1-415
1-385
31-385
1-200
C
vector
1-415
1-385
31-385
1-200
α-HA
Cdc11p
α-GFP
Bni5p
D
% budded cells with neck localization
100
50
0
vector
1-415
1-385
31-385
1-200
Cdc10p
Bni5p
Cdc11p
E
vector
1-415
1-385
F
WT
vector
1-415
1-385
31-385
1-200
YEPG
YEPD
G
total lysates
α-HA IP
no HA tag
1-415
1-385
no HA tag
1-415
1-385
: Cdc11p-HA3
α-myc
Cdc3p
α-HA
Cdc11p

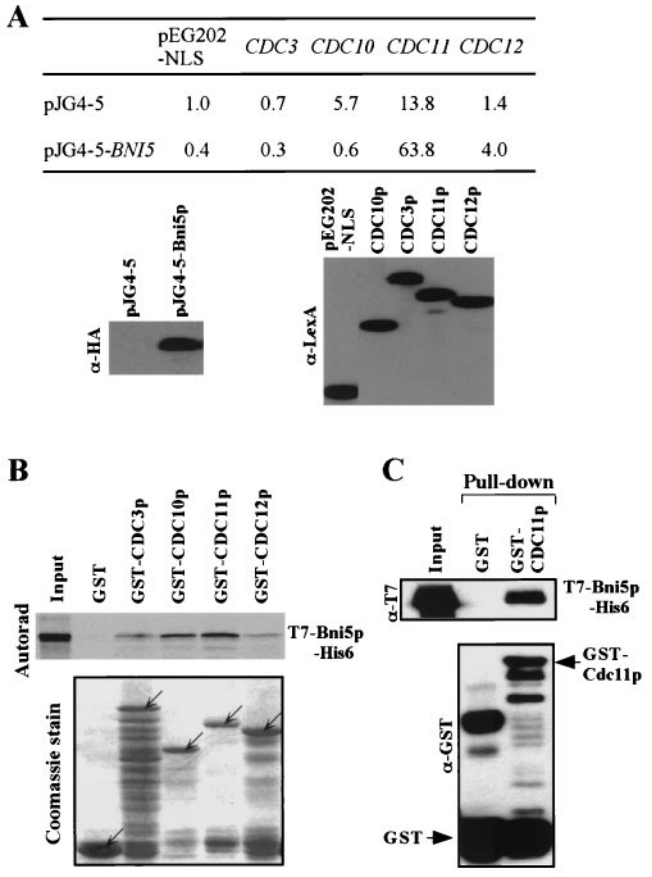

FIG. 7. Physical interactions between Bni5p and septins. (A) Two-hybrid assays were conducted as described in Materials and Methods with plasmids that expressed the full-length genes as AD or DBD fusions. Numbers indicate the Miller units of β-galactosidase activity averaged from two independent experiments. Immunoblotting (lower panels) indicated that the four septin fusions were expressed equally. (B) In vitro binding studies were carried out with ^{35}S-labeled, in vitro-translated T7-Bni5p-His$_6$ and bacterially expressed, bead-bound GST and GST-septin fusion proteins (see Materials and Methods). After pull-down, proteins were separated by SDS-PAGE. The gel was stained with Coomassie to detect GST and GST-septin fusion proteins (lower panel) and then subjected to autoradiography to detect bound Bni5p (upper panel). Note that although there was considerable degradation of the fusion proteins (particularly GST-Cdc3p), approximately equal amounts of the full-length fusion proteins were still present (arrows). Input, 2% of the ^{35}S-labeled T7-Bni5p-His$_6$ that was added to each binding reaction. (C) In vitro binding studies were carried out with bacterially expressed T7-Bni5p-His$_6$ and bead-bound GST-Cdc11p or GST (see Materials and Methods). After SDS-PAGE, the amounts of bound T7-Bni5p-His$_6$ were determined by immunoblotting with an anti-T7 antibody (upper panel), while the amounts of GST or GST-Cdc11p were determined by immunoblotting with an anti-GST antibody (lower panel). Input (upper panel), 5% of the T7-Bni5p-His$_6$ that was incubated with GST or GST-Cdc11p.

other clues to Bni5p function. Nonetheless, the *bni5*Δ mutant phenotype and the timing and pattern of Bni5p localization allow some speculations about possible functions of this protein. Because Bni5p localizes to the neck only after the septins are already there, it cannot be involved in their initial recruitment or assembly. However, the partial loss of septin localization and aberrant septin rings that are observed in the *bni5*Δ mutant suggest that Bni5p, like Gin4p, Cla4p, Elm1p, and Nap1p (7, 40, 42), contributes to the organization and/or stability of the septin array. Although the precise nature of the role of Bni5p is not yet clear, one interesting possibility is suggested by a comparison of previous electron and light microscopic observations. Byers and Goetsch observed that the apparent septin filaments were not fully evident by electron microscopy until the bud had emerged and that they seemed to disappear before cytokinesis (9, 10). However, studies using immunofluorescence and GFP-tagged proteins have shown that the septin proteins arrive at the presumptive bud site 10 to 15 min before bud emergence and typically remain at the division site for some time after cytokinesis and cell separation are complete (21, 33, 36). Thus, the localization of Bni5p to the neck at about the time of bud emergence and its abrupt disappearance just before cytokinesis suggest that it might be involved in the assembly of the higher-order septin structure that gives the appearance of filaments in the electron microscope. Because it does not appear that this higher-order structure is necessary for most aspects of septin function (22, 40), the nonlethality of the *bni5*Δ mutation is consistent with this hypothesis.

Another interesting possibility is suggested by the recent evidence that activation of the GTPase Tem1p triggers splitting of the septin array, an event that immediately precedes, and may be a prerequisite for, contraction of the actomyosin ring during cytokinesis (38). Thus, the timing of Bni5p delocalization suggests that it might be a Tem1p target, the dissociation of which from the septins is necessary for the splitting of the septin array. However, Tem1p presumably has at least one other relevant target, because most cells of a *bni5*Δ mutant appear to have a continuous septin array and to complete cytokinesis normally.

In elucidating the role(s) of Bni5p, it will also be necessary to account for the apparent lack of Bni5p homologues in other organisms. Particularly striking is the lack of an unequivocal homologue in *Candida albicans*, which also reproduces by budding and has a septin family whose sequences and assembly seem very similar to those in *S. cerevisiae* (15, 23, 57). However, it remains possible that improvements in the annotation of the *C. albicans* sequence will resolve this apparent paradox.

Roles of the predicted coiled-coil domains in septin assembly and function. Most of the known septins contain predicted coiled-coil domains at or near their C termini (39), and one simple model for septin assembly suggested that these domains might function in the formation of septin homodimers that were subunits of the heteromeric complexes (19). This model is difficult to reconcile with the dimensions of septin complexes isolated from *cdc10*Δ and *cdc11*Δ strains (22). In addition, we have shown here that Cdc11p$^{1-385}$ (which lacks the leucine zipper motif that comprises about half of the predicted coiled-coil domain) is able to associate with Cdc3p and localize apparently normally to the mother-bud neck. Moreover, in two-hybrid tests, a fragment of Cdc11p lacking the entire predicted coiled-coil domain was able to self-associate, whereas a fragment of 74 amino acids that included the entire 57-amino-acid predicted coiled-coil domain was not. Indeed, taken as a whole, the two-hybrid data (see also reference 14) suggest that the assembly of septin complexes involves a complicated set of both homomeric and heteromeric interactions that involve both the N-terminal and C-terminal domains. Higher-resolu-

tion structural data will presumably be necessary to clarify the details of septin complex assembly.

The septin coiled-coil domains may also be involved in interactions with the many proteins that are recruited to the neck in a septin-dependent manner (26). In this regard, however, it is striking that Cdc11p$^{1\text{-}385}$ was able not only to recruit Bni5p to the neck but also to rescue fully the growth defect of a *cdc11*Δ mutant. In addition, the two-hybrid data suggest that the coiled-coil domain of Cdc12p may be involved both in homomeric interactions and in interactions with the coiled-coil domain of Cdc3p. Additional structure-function studies of the various septins and the septin-interacting proteins will be necessary to clarify these issues.

ACKNOWLEDGMENTS

We are grateful to Christine Field and Jeremy Thorner for valuable discussions; Yeon-Sun Seong, Young-Wook Cho, and Dan Ilkovitch for technical support; and Jason Chong for assistance in the initial identification of *BNI5*. We also thank Susan Garfield for helping with confocal microscopy and Jim McNally and Tatiana Karpova for processing confocal images obtained at the LRBGE Fluorescence Imaging Facility at NCI.

This work was supported in part by grants NIH GM59964 (R.L.) and NIH GM31006 (J.R.P.).

P.R.L., S.S., and H.-S.R. contributed equally to this work.

ADDENDUM IN PROOF

Consistent with the results reported here, Mortensen et al. have recently noted the presence of Bni5p in isolated protein complexes that contain also the septins Gin4p and Nap1p (E. M. Mortensen, H. McDonald, J. Yates III, and D. R. Kellogg, Mol. Biol. Cell **13:**2091–2105, 2002).

REFERENCES

1. **Adams, A. E. M., and J. R. Pringle.** 1984. Relationship of actin and tubulin distribution to bud growth in wild-type and morphogenetic-mutant *Saccharomyces cerevisiae*. J. Cell Biol. **98:**934–945.
2. **Ausubel, F. M., R. Brent, R. E. Kingston, D. D. Moore, J. G. Seidman, J. A. Smith, and K. Struhl.** 1995. Current protocols in molecular biology. John Wiley and Sons, Ltd., New York, N.Y.
3. **Barral, Y., V. Mermall, M. S. Mooseker, and M. Snyder.** 2000. Compartmentalization of the cell cortex by septins is required for maintenance of cell polarity in yeast. Mol. Cell **5:**841–851.
4. **Barral, Y., M. Parra, S. Bidlingmaier, and M. Snyder.** 1999. Nim1-related kinases coordinate cell cycle progression with the organization of the peripheral cytoskeleton in yeast. Genes Dev. **13:**176–187.
5. **Bi, E., P. Maddox, D. J. Lew, E. D. Salmon, J. N. McMillan, E. Yeh, and J. R. Pringle.** 1998. Involvement of an actomyosin contractile ring in *Saccharomyces cerevisiae* cytokinesis. J. Cell Biol. **142:**1301–1312.
6. **Boeke, J. D., F. Lacroute, and G. R. Fink.** 1984. A positive selection for mutants lacking orotidine-5′-phosphate decarboxylase activity in yeast: 5-fluoro-orotic acid resistance. Mol. Gen. Genet. **197:**345–346.
7. **Bouquin, N., Y. Barral, R. Courbeyrette, M. Blondel, M. Snyder, and C. Mann.** 2000. Regulation of cytokinesis by the Elm1 protein kinase in *Saccharomyces cerevisiae*. J. Cell Sci. **113:**1435–1445.
8. **Bourne, H. R., D. A. Sanders, and F. McCormick.** 1991. The GTPase superfamily: conserved structure and molecular mechanism. Nature **349:**117–127.
9. **Byers, B.** 1981. Cytology of the yeast life cycle, p. 59–96. *In* J. N. Strathern, E. W. Jones, and J. R. Broach (ed.), The molecular biology of the yeast *Saccharomyces*: life cycle and inheritance. Cold Spring Harbor Laboratory, Cold Spring Harbor, N.Y.
10. **Byers, B., and L. Goetsch.** 1976. A highly ordered ring of membrane-associated filaments in budding yeast. J. Cell Biol. **69:**717–721.
11. **Carroll, C. W., R. Altman, D. Schieltz, J. R. Yates, and D. Kellogg.** 1998. The septins are required for the mitosis-specific activation of the Gin4 kinase. J. Cell Biol. **143:**709–717.
12. **Chant, J., M. Mischke, E. Mitchell, I. Herskowitz, and J. R. Pringle.** 1995. Role of Bud3p in producing the axial budding pattern of yeast. J. Cell Biol. **129:**767–778.
13. **DeMarini, D. J., A. E. M. Adams, H. Fares, C. De Virgilio, G. Valle, J. S. Chuang, and J. R. Pringle.** 1997. A septin-based hierarchy of proteins required for localized deposition of chitin in the *Saccharomyces cerevisiae* cell wall. J. Cell Biol. **139:**75–93.
14. **De Virgilio, C., D. J. DeMarini, and J. R. Pringle.** 1996. *SPR28*, a sixth member of the septin gene family in *Saccharomyces cerevisiae* that is expressed specifically in sporulating cells. Microbiology **142:**2897–2905.
15. **DiDomenico, B. J., N. H. Brown, J. Lupisella, J. R. Greene, M. Yanko, and Y. Koltin.** 1994. Homologs of the yeast neck filament associated genes: isolation and sequence analysis of *Candida albicans CDC3* and *CDC10*. Mol. Gen. Genet. **242:**689–698.
16. **Edgington, N. P., M. J. Blacketer, T. A. Bierwagen, and A. M. Myers.** 1999. Control of *Saccharomyces cerevisiae* filamentous growth by cyclin-dependent kinase Cdc28. Mol. Cell. Biol. **19:**1369–1380.
17. **Fares, H., L. Goetsch, and J. R. Pringle.** 1996. Identification of a developmentally regulated septin and involvement of the septins in spore formation in *S. cerevisiae*. J. Cell Biol. **132:**399–411.
18. **Field, C., R. Li, and K. Oegema.** 1999. Cytokinesis in eukaryotes: a mechanistic comparison. Curr. Opin. Cell Biol. **11:**68–80.
19. **Field, C. M., O. Al-Awar, J. Rosenblatt, M. L. Wong, B. Alberts, and T. J. Mitchison.** 1996. A purified *Drosophila* septin complex forms filaments and exhibits GTPase activity. J. Cell Biol. **133:**605–616.
20. **Field, C. M., and D. Kellogg.** 1999. Septins: cytoskeletal polymers or signalling GTPases? Trends Cell Biol. **9:**387–394.
21. **Ford, S. K., and J. R. Pringle.** 1991. Cellular morphogenesis in the *Saccharomyces cerevisiae* cell cycle: localization of the *CDC11* gene product and the timing of events at the budding site. Dev. Genet. **12:**281–292.
22. **Frazier, J. A., M. L. Wong, M. S. Longtine, J. R. Pringle, M. Mann, T. J. Mitchison, and C. Field.** 1998. Polymerization of purified yeast septins: evidence that organized filament arrays may not be required for septin function. J. Cell Biol. **143:**737–749.
23. **Gale, C., M. Gerami-Nejad, M. McClellan, S. Vandoninck, M. S. Longtine, and J. Berman.** 2001. *Candida albicans* Int1p interacts with the septin ring in yeast and hyphal cells. Mol. Biol. Cell **12:**3538–3549.
24. **Gietz, R. D., and A. Sugino.** 1988. New yeast-*Escherichia coli* shuttle vectors constructed with in vitro mutagenized yeast genes lacking six-base pair restriction sites. Gene **74:**527–534.
25. **Giot, L., and J. B. Konopka.** 1997. Functional analysis of the interaction between Afr1p and the Cdc12p septin, two proteins involved in pheromone-induced morphogenesis. Mol. Biol. Cell **8:**987–998.
26. **Gladfelter, A. S., J. R. Pringle, and D. J. Lew.** 2001. The septin cortex at the yeast mother-bud neck. Curr. Opin. Microbiol. **4:**681–689.
27. **Guan, K. L., and J. E. Dixon.** 1991. Eukaryotic proteins expressed in *Escherichia coli*: an improved thrombin cleavage and purification procedure of fusion proteins with glutathione *S*-transferase. Anal. Biochem. **192:**262–267.
28. **Haarer, B. K., and J. R. Pringle.** 1987. Immunofluorescence localization of the *Saccharomyces cerevisiae CDC12* gene product to the vicinity of the 10-nm filaments in the mother-bud neck. Mol. Cell. Biol. **7:**3678–3687.
29. **Hartwell, L. H.** 1971. Genetic control of the cell division cycle in yeast. IV. Genes controlling bud emergence and cytokinesis. Exp. Cell Res. **69:**265–276.
30. **Hill, J. E., A. M. Myers, T. J. Koerner, and A. Tzagoloff.** 1993. Yeast/*E. coli* shuttle vectors with multiple unique restriction sites. Yeast **2:**163–167.
31. **Kamei, T., K. Tanaka, T. Hihara, M. Umikawa, H. Imamura, M. Kikyo, K. Ozaki, and Y. Takai.** 1998. Interaction of Bnr1p with a novel Src homology 3 domain-containing Hof1p. Implication in cytokinesis in *Saccharomyces cerevisiae*. J. Biol. Chem. **273:**28341–28345.
32. **Kartmann, B., and D. Roth.** 2001. Novel roles for mammalian septins: from vesicle trafficking to oncogenesis. J. Cell Sci. **114:**839–844.
33. **Kim, H. B., B. K. Haarer, and J. R. Pringle.** 1991. Cellular morphogenesis in the *Saccharomyces cerevisiae* cell cycle: localization of the *CDC3* gene product and the timing of events at the budding site. J. Cell Biol. **112:**535–544.
34. **Lee, K. S., T. Z. Grenfell, F. R. Yarm, and R. L. Erikson.** 1998. Mutation of the polo-box disrupts localization and mitotic functions of the mammalian polo kinase Plk. Proc. Natl. Acad. Sci. USA **95:**9301–9306.
35. **Lee, K. S., and D. E. Levin.** 1992. Dominant mutations in a gene encoding a putative protein kinase (*BCK1*) bypass the requirement for a *Saccharomyces cerevisiae* protein kinase C homolog. Mol. Cell. Biol. **12:**172–182.
36. **Lippincott, J., and R. Li.** 1998. Dual function of Cyk2, a cdc15/PSTPIP family protein, in regulating actomyosin ring dynamics and septin distribution. J. Cell Biol. **143:**1947–1960.
37. **Lippincott, J., and R. Li.** 1998. Sequential assembly of myosin II, an IQGAP-like protein, and filamentous actin to a ring structure involved in budding yeast cytokinesis. J. Cell Biol. **140:**355–366.
38. **Lippincott, J., K. B. Shannon, W. Shou, R. J. Deshaies, and R. Li.** 2001. The Tem1 small GTPase controls actomyosin and septin dynamics during cytokinesis. J. Cell Sci. **114:**1379–1386.
39. **Longtine, M. S., D. J. DeMarini, M. L. Valencik, O. S. Al-Awar, H. Fares, C. De Virgilio, and J. R. Pringle.** 1996. The septins: roles in cytokinesis and other processes. Curr. Opin. Cell Biol. **8:**106–119.
40. **Longtine, M. S., H. Fares, and J. R. Pringle.** 1998. Role of the yeast Gin4p

protein kinase in septin assembly and the relationship between septin assembly and septin function. J. Cell Biol. **143:**719–736.
41. **Longtine, M. S., A. McKenzie III, D. J. Demarini, N. G. Shah, A. Wach, A. Brachat, P. Philippsen, and J. R. Pringle.** 1998. Additional modules for versatile and economical PCR-based gene deletion and modification in *Saccharomyces cerevisiae*. Yeast **14:**953–961.
42. **Longtine, M. S., C. L. Theesfeld, J. N. McMillan, E. Weaver, J. R. Pringle, and D. J. Lew.** 2000. Septin-dependent assembly of a cell cycle-regulatory module in *Saccharomyces cerevisiae*. Mol. Cell. Biol. **20:**4049–4061.
43. **Lupas, A.** 1996. Coiled coils: new structures and new functions. Trends Biochem. Sci. **21:**375–382.
44. **Lupas, A., M. V. Dyke, and J. Stock.** 1991. Predicting coiled coils from protein sequences. Science **252:**1162–1164.
45. **Mino, A., K. Tanaka, T. Kamei, M. Umikawa, T. Fujiwara, and Y. Takai.** 1998. Shs1p: a novel member of septin that interacts with Spa2p, involved in polarized growth in *Saccharomyces cerevisiae*. Biochem. Biophys. Res. Commun. **251:**732–736.
46. **Sherman, F., G. R. Fink, and J. B. Hicks.** 1986. Methods in yeast genetics. Cold Spring Harbor Laboratory Press, Cold Spring Harbor, N.Y.
47. **Shulewitz, M. J., C. J. Inouye, and J. Thorner.** 1999. Hsl7 localizes to a septin ring and serves as an adapter in a regulatory pathway that relieves tyrosine phosphorylation of Cdc28 protein kinase in *Saccharomyces cerevisiae*. Mol. Cell. Biol. **19:**7123–7137.
48. **Sikorski, R. S., and P. Hieter.** 1989. A system of shuttle vectors and yeast host strains designed for efficient manipulation of DNA in *Saccharomyces cerevisiae*. Genetics **122:**19–27.
49. **Siliciano, P. G., and K. Tatchell.** 1984. Transcription and regulatory signals at the mating type locus in yeast. Cell **37:**969–978.
50. **Song, S., T. Z. Grenfell, S. Garfield, R. L. Erikson, and K. S. Lee.** 2000. Essential function of the polo box of Cdc5 in subcellular localization and induction of cytokinetic structures. Mol. Cell. Biol. **20:**286–298.
51. **Song, S., and K. S. Lee.** 2001. A novel function of *Saccharomyces cerevisiae CDC5* in cytokinesis. J. Cell Biol. **152:**451–469.
52. **Spellman, P. T., G. Sherlock, M. Q. Zhang, V. R. Iyer, K. Anders, M. B. Eisen, P. O. Brown, D. Botstein, and B. Futcher.** 1998. Comprehensive identification of cell cycle-regulated genes of the yeast *Saccharomyces cerevisiae* by microarray hybridization. Mol. Biol. Cell **9:**3273–3297.
53. **Straight, A. F., W. F. Marshall, J. W. Sedat, and A. W. Murray.** 1997. Mitosis in living budding yeast: anaphase A but no metaphase plate. Science **277:**574–578.
54. **Takizawa, P. A., J. L. DeRisi, J. E. Wilhelm, and R. D. Vale.** 2000. Plasma membrane compartmentalization in yeast by messenger RNA transport and a septin diffusion barrier. Science **290:**341–344.
55. **Vallen, E. A., J. Caviston, and E. Bi.** 2000. Roles of Hof1p, Bni1p, Bnr1p, and Myo1p in cytokinesis in *Saccharomyces cerevisiae*. Mol. Biol. Cell **11:**593–611.
56. **Waddle, J. A., T. S. Karpova, R. H. Waterston, and J. A. Cooper.** 1996. Movement of cortical actin patches in yeast. J. Cell Biol. **132:**861–870.
57. **Warenda, A. J., and J. B. Konopka.** Septin function in *Candida albicans* morphogenesis. Mol. Biol. Cell **13:**2732–2746.